



1 **Comparing hydrological modelling, linear and multilevel**
2 **regression approaches for predicting baseflow index for 596**
3 **catchments across Australia**

4 Junlong Zhang^{1,2}, Yongqiang Zhang^{1*}, Jinxi Song^{2,3}, Lei Cheng¹, Rong Gan¹,

5 Xiaogang Shi⁴, Zhongkui Luo⁵, Panpan Zhao⁶

6 ¹ CSIRO Land and Water, GPO Box 1700, ACTON 2601, Canberra, Australia

7 ² Shaanxi Key Laboratory of Earth Surface System and Environmental Carrying Capacity,
8 College of Urban and Environmental Sciences, Northwest University, Xi'an 710127, China

9 ³ State Key Laboratory of Soil Erosion and Dryland Farming on the Loess Plateau, Institute
10 of Soil and Water Conservation, Chinese Academy of Sciences, Yangling 712100, China

11 ⁴ Lancaster Environment Centre, Lancaster University, Lancaster, UK, LA1 4YQ

12 ⁵ CSIRO Agriculture Flagship, GPO Box 1666, ACTON 2601, Canberra, Australia

13 ⁶ State Key Laboratory of Hydrology-Water Resource and Hydraulic Engineering, College of
14 Hydrology and Water Resources, Hohai University, Nanjing 210098, China

15 Submission to: Hydrology and Earth System Sciences

16 *Corresponding author: Yongqiang Zhang

17 CSIRO Land and Water, Clunies Ross Street, Canberra 2601, Australia

18 E-mail: yongqiang.zhang@csiro.au; Tel.: +61 2 6246 5761; Fax: +61 2 6246 5800



19 **Abstract.** Estimating baseflow at a large spatial scale is critical for water balance budget, water
20 resources management, and environmental evaluation. To predict baseflow index (BFI, the
21 ratio of baseflow to total streamflow), this study introduces a multilevel regression approach,
22 which is compared to two traditional approaches: hydrological modelling (SIMHYD, a
23 simplified version of the HYDROLOG model, and Xinanjiang models) and classic linear
24 regression. All of the three approaches were evaluated against ensemble average estimates from
25 four well-parameterised baseflow separation methods (Lyne-Hollick, UKIH (United Kingdom
26 Institute of Hydrology), Chapman-Maxwell and Eckhardt) at 596 widely spread Australian
27 catchments in 1975-2012. The two hydrological models obtain BFI from three modes:
28 calibration and two regionalisation schemes (spatial proximity and integrated similarity). The
29 classic linear regression estimates BFI using linear regressions established between catchment
30 attributes and the ensemble average estimates in four climate zones (arid, tropics, equiseasonal
31 and winter rainfall). The multilevel regression approach not only groups the catchments into
32 the four climate zones, but also considers variances both within all catchments and catchments
33 in each climate zone. The two calibrated and regionalised hydrological models perform
34 similarly poorly in predicting BFI with a Nash-Sutcliffe Efficiency (NSE) of -8.44~-2.58 and
35 an absolute percent bias (Bias) of 81~146; the classic linear regression is intermediate with
36 the NSE of 0.57 and bias of 25; the multilevel regression approach is best with the NSE of 0.75
37 and bias of 19. Our study indicates the multilevel regression approach should be used for
38 predicting large-scale baseflow index such as Australian continent where sufficient catchment
39 predictors are available.

40 **Keywords:** baseflow separation, baseflow index, hydrological models, linear regression,
41 multilevel regression, Australia



42 **Highlights**

- 43 1. The multilevel regression approach is introduced for predicting baseflow index
- 44 2. The hydrological modelling approach overestimates baseflow in Australia
- 45 3. The multilevel regression approach is best in arid, tropics, and equiseasonal regions
- 46 4. The linear regression approach performs similarly to the multilevel regression
- 47 approach in winter rainfall region



48 **1 Introduction**

49 Baseflow, the outflow from the upstream aquifers when the recharge is ceased (e.g.,
50 precipitation or other artificial water supplies) (Brutsaert and Lopez, 1998; Brutsaert, 2005),
51 is an important indicator of catchment hydrogeological characteristic (Knisel, 1963).
52 Baseflow index (BFI) is the average rate of baseflow to streamflow over a long period of time
53 (Piggott et al., 2005; Partington et al., 2012). Accurate estimation of baseflow and BFI has
54 profound influence on sustaining water for basins during drought periods (Brutsaert,
55 2005; Miller et al., 2016), and therefore is critical for water budgets (Abdulla et al., 1999),
56 water management strategies (Lacey and Grayson, 1998), engineering design (Meynink,
57 2011), and environmental issues (Spongberg, 2000; Miller et al., 2014).
58 Various methods have been developed to separate baseflow from streamflow (Lyne and
59 Hollick, 1979; Rice and Hornberger, 1998; Spongberg, 2000; Furey and Gupta, 2001; Eckhardt,
60 2005; Tularam and Ilahee, 2008; Lott and Stewart, 2016), which can be categorized to tracer
61 based and non-tracer methods (Gonzales et al., 2009). However, tracer based method is only
62 applied to experimental catchments due to expensive the high consumption of both
63 experimental time and materials (Koskelo et al., 2012). The alternative is non-tracer methods
64 (e.g., digital filter methods) (Zhang et al., 2017), which are widely used because of their high
65 efficiency and repeatability in estimating BFI (Arnold et al., 1995). More importantly, they
66 perform well when the digital-filtering parameters (e.g., recession constant and maximum
67 baseflow index) are appropriately estimated (Zhang et al., 2017). The non-tracer methods can
68 only be used for catchments with streamflow observations. For ungauged catchments,
69 hydrological models and regression approaches can be used to separate baseflow form total
70 streamflow. Their accuracy can be evaluated against ensemble estimates from the non-tracer
71 methods at gauged catchments.



72 Most hydrological models include a baseflow generation component (Luo et al.,
73 2012;Stoelzle et al., 2015;Gusyev et al., 2016). These models can be divided into two groups.
74 One group considers baseflow as a linear recession process for groundwater reservoir,
75 including SIMHYD (simplified version of the HYDROLOG model) (Chiew and McMahon,
76 1994;Zhang et al., 2016), 1LBY (Abdulla et al., 1999;Stoelzle et al., 2015), HBV (Ferket et
77 al., 2010) models; the another group takes baseflow as a non-linear recession process
78 including Xinanajing (Zhang and Chiew, 2009), PDM (Ferket et al., 2010) and ARNO
79 (Abdulla et al., 1999) models. It is expected that BFI obtained from the hydrological models
80 is largely uncertain as a result of different model structures, model calibration and
81 parameterisation schemes (Beven and Freer, 2001). There are few studies in the literatures to
82 evaluate the accuracy of baseflow estimation from the hydrological models at a regional
83 scale. This study evaluates two hydrological models (SIMHYD and Xinanjiang models) for
84 predicting BFI against the ensemble BFI estimates from the non-tracer methods.

85 Linear regression approach is another commonly used method to predict hydrological
86 signature indices, including baseflow index (Gallart et al., 2007;Longobardi and Villani,
87 2008;Bloomfield et al., 2009;van Dijk et al., 2013). This method uses catchment physical
88 characteristics (i.e. descriptors) and BFI obtained from the gauged catchments to establish
89 linear regressions that are then used to predict BFI in ungauged catchments (Bloomfield et
90 al., 2009;Beck et al., 2013). Several studies show some catchment characteristics have
91 important control on BFI. For instance, geological characteristics such as soil properties were
92 found to be key for accurate BFI estimates (Brandes et al., 2005;van Dijk, 2010). Other
93 studies also used climate-related indices, such as mean annual precipitation and mean annual
94 potential evaporation, to simulate BFI (van Dijk, 2010;Beck et al., 2013). In similar studies,
95 mean annual precipitation, slope and proportion of grassland are used for building the
96 regressions for predicting BFI (Haberlandt et al., 2001;Brandes et al., 2005;Mazvimavi et al.,



97 2005;Gebert et al., 2007;Bloomfield et al., 2009;van Dijk, 2010). Beside BFI, linear
98 regression is also an useful approach in estimating other hydrological signatures (e.g., runoff
99 coefficient, runoff seasonality, zero flow ratio and concavity index (Zhang et al., 2014)) and
100 understanding the catchment hydrology behaviour (Zhang et al., 2014;Su et al., 2016). One
101 limitation of the linear regression approach is that it uses constant parameters to predict BFI,
102 and cannot handle cross-interactions at different spatial scales (Qian et al., 2010), which
103 could result in large errors for catchments located in a wide range of climate regimes.

104 This limitation can be overcome by the multilevel regression approach that provides a robust
105 tool to establish the relationships between BFI and catchment attributes. The basic idea of
106 this approach is that higher level variables vary within a lower level (Berk and De Leeuw,
107 2006). This approach can handle the variables with various solutions using random effects
108 (i.e., hierarchical structure) (Dudaniec et al., 2013). This approach has been extensively used
109 to understand interplay of ecosystem dynamics (i.e., carbon cycle across different ecosystem
110 (McMahon and Diez, 2007;Luo et al., 2015) and N₂O emissions from agricultural soils
111 (Carey, 2007)). However, no literatures have been reported to use this approach for
112 hydrological signature (such as BFI) predictions. This study, for the first time, explores the
113 possibility of using multilevel regression (Qian et al., 2010;Luo et al., 2015) to predict BFI
114 across widely distributed Australian catchments. Catchment characteristics are used here as
115 lower level (i.e., individual-level) predictors, and the effect of these predictors is assumed to
116 vary across higher level predictors (i.e., climate zones) (Gelman and Hill, 2006). Details of
117 the multilevel regression approach are elaborated in section 3.3.

118 The main aim of this study is to improve the large-scale BFI prediction. To achieve this, we
119 compare the three BFI prediction methods (hydrological modelling, classic and multilevel
120 regression approaches) against ensemble average estimates from four non-tracer baseflow
121 separation methods. The objectives of this study are to



- 122 i. Obtain “benchmark” BFI using the four non-tracer baseflow methods (Lyne-Hollick,
123 UKIH (United Kingdom Institute of Hydrology), Chapman-Maxwell and Eckhardt)
124 for 596 Australian catchments (Figure 1);
- 125 ii. Introduce the multilevel regression approach for FBI predictions across large regions;
- 126 iii. Assess relative merits of the three approaches for BFI predictions; and
- 127 iv. Investigate good BFI predictors for the multilevel regression approach.

128 Figure 1 is about here

129 2 Data sources

130 2.1 Streamflow

131 There are 596 catchments selected across Australia for assessing the three methods
132 (hydrological modelling, linear regression and multilevel regression) used in this study to
133 predict BFI. Streamflow measurements and related catchment attributes were collated by
134 Zhang et al. (2013). Following criteria are used to filter the streamflow data for each
135 catchment:

- 136 i. It is a small catchment with catchment area 50 to 5000 km²;
- 137 ii. Streamflow was not subject to dam or reservoir regulations;
- 138 iii. The catchment is non-nested;
- 139 iv. The catchment was not subject to major impacts of irrigation and intensive land use;
140 and
- 141 v. The observed streamflow record covers the period of 1975-2012, containing at least
142 ten-year (>3652 days) daily observations, with acceptable data quality according to a
143 consistent Australian standard.



144 2.2 Climate zones and catchment attributes

145 The Australian continent is classified into five climate zones (arid, equiseasonal-hot,
146 equiseasonal-warm, tropics and winter rainfall) based on Köppen-Geiger classification
147 schemes (Kottek et al., 2006). It is noted that this study combined equiseasonal-hot and
148 equiseasonal-warm as one climate zone. The number of selected catchments within arid,
149 equiseasonal, tropics, and winter rainfall climate zones is 37, 385, 82, and 90, respectively.

150 The catchment attributes including climate (Mean annual precipitation, Mean annual
151 potential evaporation), topographical (Mean elevation and Mean slope), soil (Available soil
152 water holding capacity) and land cover (Forest cover ratio) characteristics were implemented
153 to build the linear regression and multilevel regression approaches. The abbreviation for each
154 catchment attributes and summary are shown in Table 1 and Table 2 respectively.

155 2.3 Forcing data for hydrological modelling

156 The Xinanjaing and SIMHYD models were driven by 0.05° resolution (~ 5 km) daily
157 meteorological data (including maximum temperature, minimum temperature, incoming solar
158 radiation, actual vapour pressure and precipitation) from 1975 to 2012, obtained from the
159 SILO Data Drill of the Queensland Department of Natural Resources and Water
160 (www.nrw.gov.au/silo). There are about 4600-point observations across Australia used for
161 interpolating to obtain the SILO data. Details are described in Jeffrey et al. (2001). The daily
162 and monthly gridded precipitation data were obtained from ordinary kriging method, whereas
163 other gridded climate variables were obtained using the thin plate smoothing spline. Cross
164 validation results indicate the mean absolute error of the Jeffrey interpolation for maximum
165 daily air temperature, minimum daily air temperature, vapour pressure, and precipitation
166 being 1.0 °C, 1.4 °C, 0.15 kPa and 12.2 mm/month, which indicates good data quality
167 (Jeffrey et al., 2001).



168 Except for the climate forcing data, the two models also require remote sensing leaf area
169 index, land cover and albedo data that were used to calculate actual evapotranspiration (ET_a)
170 using the Penman–Monteith–Leuning model (Leuning et al., 2009;Zhang et al., 2010). The
171 leaf area index data from 1981 to 2011, derived from the Advanced Very High Resolution
172 Radiometer (AVHRR), were obtained from Boston University (Zhu et al., 2013). The
173 temporal resolution is half–monthly and its spatial resolution is ~8 km. The land cover data
174 required to estimate aerodynamic conductance came from the 2000-2001 MODIS land cover
175 product, obtained from the Oak Ridge National Laboratory Distributed Active Archive
176 Center (Friedl et al., 2010). The dataset has 17 vegetation classes, which are defined
177 according to the International Geosphere-Biosphere Programme. The albedo data required to
178 calculate net radiation were obtained from the 8-day MODIS MCD43B bidirectional
179 reflectance distribution function product at 1 km resolution. All of the forcing data were re-
180 projected and resampled using nearest neighbour approach to obtain 0.05° gridded data.

181 **3 Models**

182 3.1 Baseflow separation algorithm

183 The benchmark BFI data were estimated using four baseflow separation methods. They are
184 Lyne-Hollick (Lyne and Hollick, 1979), UKIH (Gustard et al., 1992), Chapman-Maxwell
185 (Chapman and Maxwell, 1996) and Eckhardt (Eckhardt, 2005) respectively. It is found that
186 estimates of the recession constant and maximum baseflow index are the key to improve the
187 performance of the digital-filtering methods (Zhang et al., 2017). This study used the
188 Automatic Baseflow Identification Technique (ABIT) for the recession analysis, which was
189 developed by Cheng et al. (2016) based on the recession theory provided by Brutsaert and
190 Nieber (1977). Figure 2 demonstrates how the recession constant is estimated using the ABIT
191 method.



192 In order to eliminate uncertainties raised from different algorithms, the ensemble mean from
193 the four methods was taken as the benchmark (denoted as ‘the observed BFI’). The observed
194 BFI was used either to evaluate the two hydrological models for BFI prediction, or to build
195 the linear and multilevel regression approaches together with the catchment attributes.

196 Figure 2 is about here

197 3.2 Hydrological models

198 The SIMHYD and Xinanjiang model are two conceptual rainfall-runoff hydrological models.
199 Since developed by Chiew and McMahon (2002), SIMHYD has been widely applied in
200 runoff simulation and regionalization studies (Chiew et al., 2009; Vaze and Teng, 2011; Li and
201 Zhang, 2016; Zhang et al., 2016). Four water stores are used in this model to describe
202 hydrological processes, namely the interception store, soil moisture store, groundwater store
203 and channel store (Chiew and McMahon, 2002). Detailed model structure can be found in
204 Chiew and McMahon (1994). The modified SIMHYD model by Zhang and Chiew (2009),
205 which uses remote sensing data and contains nine model parameters, is used in this study.

206 The Xinanjiang model was developed by Zhao (1992) and has been widely used in humid
207 and semi-humid regions (Li et al., 2009; Lü et al., 2013; Yao et al., 2014). This model
208 reproduces runoff by describing three hydrological processes including ET_a , runoff
209 generation, and runoff routing. Details of Xinanjiang model are available from studies
210 conducted by Zhao (1992) and Zhang and Chiew (2009). Here we use the modified
211 Xinanjiang model proposed by Zhang and Chiew (2009), in which ET_a was estimated using
212 remote sensed LAI and the model parameters were reduced from 14 to 12.

213 The revised version of those two models is denoted as original models. The details of two
214 hydrological models and regionalization approaches are described by Zhang and Chiew
215 (2009). We used three types of BFI estimates from hydrological modelling: calibration,



216 regionalisation from spatial proximity, and regionalisation from integrated similarity. Herein,
217 a short description of these three kinds of estimates is given below.

218 For model calibration, a global optimisation method, the genetic algorithm from the global
219 optimisation toolbox in MATLAB (MathWorks, 2006), was used to calibrate the model
220 parameters for each catchment. This optimiser used 400 populations and the maximum
221 generation of 100 for searching the optimum point, which converges at approximately 50
222 generations of searching. The model calibration was to maximise the Nash-Sutcliffe
223 Efficiency of the daily square-root-transformed runoff data and minimise the model bias (Li
224 and Zhang, 2017).

225 For the spatial cross-validations, two regionalisation approaches, spatial proximity and
226 integrated similarity approaches (Zhang and Chiew, 2009) were used. The spatial proximity
227 approach is where the geographically closest catchment is used as the donor basin to predict
228 the ungauged catchments; integrated similarity approach is derived from combination of the
229 spatial proximity and physical similarity approaches.

230 3.3 Linear regression and multilevel regression approaches

231 Traditionally, BFI was predicted using one set parameters for all catchments. The details are:

$$232 \quad BFI_i = N(\alpha + \beta \cdot X_i, \varepsilon), i = 1, 2, 3, \dots, 596, \quad (1)$$

233 where BFI_i is the baseflow index for each catchment $i=1, \dots, 596$, N is normal distribution
234 function, α is the intercept, β is slop, X is the variables (i.e., catchment attributes), and ε is
235 variance. This model ignores the potentially different effects of the same variable on BFI
236 across different climatic zones. That is, α and β are constant irrespective of the climatic zone
237 to which the BFI belongs. To be specific, many studies have conducted the baseflow
238 prediction at large area, yet constant α and β are used in the model (Abebe and Foerch,



239 2006;Longobardi and Villani, 2008;Bloomfield et al., 2009). However, catchment attributes
240 vary with hydrometeorological conditions, therefore the constant parameters are not adequate
241 to reflect the catchment characteristics. This approach ignored variability of catchment
242 characteristics in various backgrounds. In order to reduce the uncertainties of prediction using
243 one set of parameters, one level reflects hydrological background should be introduced.

244 In this study, we assumed that BFI associates with the climate variables (annual precipitation,
245 potential evapotranspiration) and terrain attributes (area, elevation, slope, land cover and
246 available soil water holding capacity in top soil) in each catchment (i.e., $i = 1, 2, 3, \dots, 596$).
247 We further assumed that the effects of those predictors on BFI vary with climate zones
248 including arid, tropics, equiseasonal and winter rainfall (i.e., $j = 1, 2, 3, 4$). In this process, the
249 catchments were divided into multiple datasets based on climate zones, then individual linear
250 regression model were built for each subset.

$$251 \quad BFI_{j_i} = N(\alpha + \beta \cdot X_{j_i}, \varepsilon), i \in (1,2,3,\dots,n) \quad (2)$$

252 where j is catchment in each climate zone, BFI_{j_i} is the baseflow index for catchment in each
253 subset $j = 1,2,3,4$. N is normal distribution function, α is the intercept, β is slop, X is the
254 variables (i.e., catchment attributes), and ε is variance in each subset. However, hydrological
255 processes in a catchment have close connections with other catchments, interactions crossing
256 various group levels are primary drivers to influence baseflow processes. Therefore, an
257 approach should be developed to consider cross level effects for predicting hydrological
258 signatures.

259 Thus, we introduced the multilevel regression approach (Gelman and Hill, 2006;Qian et al.,
260 2010;Luo et al., 2015) to improve the prediction of BFI and quantify the relative importance
261 of predictors under different climate zones. Comparing the traditional linear regression
262 approach, the hierarchical structure of the multilevel regression approach allows the



263 assessment of the variation in model coefficients across groups (e.g., climatic zones) and
 264 accounting for group-level variation in the uncertainty for individual level coefficients. The
 265 multilevel regression approach could be written as a data-level model (the predicted BFI_{*i*}
 266 belonging to climate zone *j*), allowing the model coefficients (α and β) to vary by climate
 267 zone ($j = 1, 2, 3, 4$). In this model, the intercept and slope vary with the group level (i.g.,
 268 climate zone). The details of the approach is elaborated as follows:

$$269 \quad BFI_i \sim N(\alpha_{j[i]} + \beta_{j[i]} \cdot X_i, \sigma_{BFI}^2), i = 1, 2, 3, \dots, 596, \quad (3)$$

270 where X_i is the catchment attributes for each basin, and its intercepts and slopes can be
 271 decomposed into terms for climate zone,

$$272 \quad \begin{pmatrix} \alpha_j \\ \beta_j \end{pmatrix} \sim N \left(\begin{pmatrix} \mu_\alpha \\ \mu_\beta \end{pmatrix}, \begin{pmatrix} \sigma_\alpha^2 & \rho\sigma_\alpha\sigma_\beta \\ \rho\sigma_\alpha\sigma_\beta & \sigma_\beta^2 \end{pmatrix} \right), j = 1, 2, 3, 4, \quad (4)$$

273 where μ_α and σ_α are the mean and standard deviation of variable intercept α , μ_β and σ_β are the
 274 mean and standard deviation of variable slope β , ρ is the correlation coefficients between the
 275 two variables α_j and β_j . The Eq. (3) can be rearranged as block matrix of

$$276 \quad A \sim N(\mu, \sigma) \quad (5)$$

277 the details of Eq. (5) $A \sim N(\mu, \sigma)$ can be described as:

$$278 \quad A = \begin{pmatrix} \alpha_j \\ \beta_j \end{pmatrix}, \mu = \begin{pmatrix} \mu_\alpha \\ \mu_\beta \end{pmatrix}, \sigma = \begin{pmatrix} \sigma_\alpha^2 & \rho\sigma_\alpha\sigma_\beta \\ \rho\sigma_\alpha\sigma_\beta & \sigma_\beta^2 \end{pmatrix} \quad (6)$$

279 the Eq. (4) can be calculated individually by:

$$280 \quad \alpha_j \sim N(\mu_\alpha, \sigma_\alpha^2) \quad (7)$$

$$281 \quad \beta_j \sim N(\mu_\beta, \sigma_\beta^2) \quad (8)$$



282 The density function of the normal distribution N is (for example, α variable):

$$283 \quad f(\alpha_j) = \frac{1}{\sqrt{2\pi}\sigma_\alpha} e^{-\frac{(\alpha_j - \mu_\alpha)^2}{2\sigma_\alpha^2}} \quad (9)$$

284 This model considers variation in the α_j 's and the β_j 's and also a between-group correlation
285 parameter ρ (Gelman and Hill, 2006; Qian et al., 2010). In essence, there is a separate
286 regression model for each climate zone with the coefficients estimated by the weighted
287 average of pooled (which do not consider groups) and unpooled (which consider each group
288 separately) estimates, i.e. partial pooling. When fitting the model, all predictors are
289 standardized using *z-scores*.

$$290 \quad x' = \frac{x - \text{mean}(x)}{2SD(x)} \quad (10)$$

291 Where x' is the new catchment attributes using function *z-scores*.

292 3.4 Leave-one-out cross-validations

293 We apply leave-one-out cross-validation to assess the ability of the two regression
294 approaches to predict BFI in 'ungauged' catchments where no streamflow data are available.
295 For each of the 596 catchments, the data from other 595 catchments are used to predict its
296 BFI. This procedure is repeated over all 596 catchments. This cross-validation procedure
297 explores the transferability of the two regression approaches from known catchments to the
298 ungauged and particularly evaluates the value of the between-catchments information.

299 4 Model evaluation

300 4.1 Bias

301 The absolute percentage bias was used to evaluate model performance, which is calculated
302 as:



$$303 \quad \text{Bias} = \frac{\sum_{i=1}^n (BFI_s - BFI_o)}{\sum_{i=1}^n BFI_o} \times 100 \quad (11)$$

304 where BFI_o is the observed BFI derived using the ensemble average from the four non-tracer
 305 baseflow separation approaches (i.e., Lyne-Hollick, UKIH, Chapman-Maxwell and
 306 Eckhardt), BFI_s is the simulated BFI from the two hydrological models or the two regression
 307 approaches. And n is the total number of catchment. The unit of bias is a percentage (%), the
 308 larger of the absolute bias, the worse of the simulation. The bias is 0 indicates that simulated
 309 value is the same as the observed value.

310 4.2 Nash-Sutcliffe efficiency (NSE)

$$311 \quad NSE = 1 - \frac{\sum_{i=1}^n (BFI_o - BFI_s)^2}{\sum_{i=1}^n (BFI_o - \overline{BFI_s})^2} \quad (12)$$

312 The Nash-Sutcliffe efficiency (NSE) is a normalized statistic that measures the relative
 313 magnitude of the residual variance ("noise") compared to the measured data variance
 314 ("information") (Nash and Sutcliffe, 1970). It is a classic statistical metrics used for
 315 evaluating the model performance. The closer NSE is to 1.0, the better the simulation is.

316 5 Results

317 5.1 Spatiality of observed BFI

318 It can be seen from Figure 3 that BFI varies dramatically across Australia (location, i.e.
 319 coordination and distance away from ocean). Within the latitude ranges from 20°S to 30°S,
 320 which is smaller than that of the regions beyond this latitude range. Catchments located in
 321 latitudes higher than 30°S tend to have larger BFIs in general. Yet this is not the case for



322 Tasmania, where catchments with latitude higher than 40°S have smaller BFI values in the
323 southeastern region within this island. This indicates that the BFI spatiality is distinct from
324 the main continent to island. It is also interesting to notice that beyond the range of 20-30°S,
325 observed BFI increases from inner land to coastal catchments, especially in southeast region
326 within the main Australian continent.

327 Figure 3 is about here

328 5.2 Performance of two hydrological models

329 Figure 4 summarises the BFI duration curves generated from the two hydrological models
330 with three modes (calibration and two regionalisation schemes). Both models in the three
331 parameterisation schemes perform poorly for estimating BFI. SIMHYD model largely
332 overestimates BFI, while Xinanjiang model is overestimated at 60 % catchments, and its
333 estimated BFI is closer to the observed that that obtained from SIMHYD model. Differences
334 among the calibration and two regionalisation schemes are marginal for both models.

335 Figure 4 is about here

336 We further compared the observed and simulated in scatterplots (Figure 5). Figure 5(a) and
337 5(d) compares the observed and simulated BFIs from calibrated SIMHYD and Xinanjiang
338 models, respectively. Figure 5(b)-(c) and 5(e)-(f) show the regionalisation results (i.e., spatial
339 proximity and integrated similarity) of these two hydrological models. Notably, BFI
340 estimated using SIMHYD model is much larger than the observed values (Figure 5(a), (b),
341 and (c)), with the majority catchment BFIs dotted above the 1:1 line. SIMHYD model under
342 calibration, spatial proximity, and integrated similarity gives NSE being -8.30, -8.42 and -
343 8.44 respectively, and gives percentage bias being 146, 152 and 152 respectively, indicating
344 similar poor model performance. In comparison, BFI estimated from Xinanjiang model tends
345 to scatter a larger range around 1:1 line regardless of the parameterisation method (Figure



346 5(d), (e), and (f)), and is closer to the observed BFI. Xinanjiang model under calibration,
347 spatial proximity, and integrated similarity give NSE being -2.75, -2.70 and -2.58
348 respectively, and gives bias being 84, 81 and 83 respectively, indicating still similar poor
349 model performance in prediction of BFI. The results obtained from Figures 4 and 5 indicate
350 that parameterisation has much smaller impact on BFI estimates, compared to model
351 structure.

352 Figure 5 is about here

353 5.3 Comparison of traditional regression and multilevel regression approaches

354 Figure 6 compares the observed BFIs and simulated BFIs using traditional linear multivariate
355 regression and multilevel regression approaches across four different climate zones. The
356 result shows that the multilevel regression approach generally outperforms the traditional
357 linear regression approach, evidenced by the NSE from multilevel regression approach being
358 0.31, 0.30, and 0.18 higher than that from linear regression in arid, tropics, and equiseasonal
359 regimes respectively, and the percentage bias from multilevel regression approach being 8,
360 7, and 8 lower than that from the linear regression. The two approaches show no significant
361 difference in winter rainfall climate zone, indicated by same bias or NSE.

362 Figure 6 is about here

363 We further check the leave-one-out cross-validation results obtained from the two approaches
364 (Figure 7). It is clear that there exists noticeable degradation from calibration to cross
365 validations for the traditional regression in the three climate zones: arid, tropics, and
366 equiseasonal regimes. Compared to that, there is no noticeable degradation for the multilevel
367 regression approach for the three climate zones. In the winter rainfall zone, the both
368 approaches do not have degradation, and perform similarly. The leave-one-out cross-



369 validation results further demonstrate the multilevel regression approach outperforms the
370 traditional linear regression.

371 Figure 7 is about here

372 Figure 8 summarises parameters of the multilevel regression approach. It can be seen that
373 precipitation has the most positive impact on BFI, which does not greatly vary across climate
374 zones. E_{TP} has the most negative effect among all climate zones, and has significant large
375 effect in equiseasonal zone. The H and Kst also have the noticeable positive effect on all the
376 climate zones. Other three characteristics A, S and F have slope close to zero, suggesting
377 small impacts on BFI.

378 Figure 8 is about here

379 **6 Discussion**

380 Our results suggest there are large biases to use hydrological models to simulate and predict
381 BFI. It is understandable since hydrological models are not designed to simulate baseflow
382 directly, but the baseflow component, in order to better simulate streamflow. It seems that
383 model structure is more important than parameterisation since the three parameterisation
384 schemes (calibration, spatial proximity and integrated similarity) obtain similar BFI, and
385 SIMHYD has larger bias than Xinanjiang model as summarised in Figures 4 and 5. However,
386 both hydrological models are calibrated against total streamflow, rather than its components,
387 such as baseflow. This suggests that better estimate streamflow. This issue has been well
388 recognised in other hydrological models as well (Fenicia et al., 2007; Lo et al., 2008). In fact,
389 baseflow is designed as an integrated store combined with the river recharge (Chiew and
390 McMahon, 2002). This structure feature of hydrological models tends to overestimate
391 baseflow and therefore leads to unsatisfactory BFI prediction.



392 Interactions of catchments crossing group level would influence the baseflow processes. BFI
393 is affected by catchment attributes, and in relevance with terrain and climate factors (Gustard
394 and Irving, 1994; Longobardi and Villani, 2008; van Dijk, 2010; Price, 2011). However, how
395 to predict the effect of BFI response to such various environmental conditions remains
396 challenging. In order to improve our understanding of BFI, interaction of catchment attributes
397 within different climate zones should be considered (Berk and De Leeuw, 2006).

398 Climate influences the hydrological process and thus leads to changes in baseflow generation.
399 Implementation of multilevel regression approach in this study, P and E_{TP} have the most
400 significant effects on BFI, are the two essential elements controlling baseflow processes. The
401 effect of these two factors varies across climate zones. As studies by Santhi et al. (2008) and
402 Peña-Arancibia et al. (2010), they have shown that climate attributes can be used to best
403 predictors for recession constant. The increase of the precipitation can cause the more
404 saturation of the soil, and lead to the baseflow increase (Mwakalila et al., 2002; Abebe and
405 Foerch, 2006). In addition, the E_{TP} is related to the baseflow discharge over the extended
406 period (Wittenberg and Sivapalan, 1999). E_{TP} has the adverse effect on BFI for all climate
407 zones. This result agrees well with the conclusion drawn by Mwakalila et al. (2002). The
408 influence is relative smaller in arid zone than other climate zones. In general, E_{TP} is related to
409 the baseflow discharge over the extended period (Wittenberg and Sivapalan, 1999),
410 catchment with low evapotranspiration will have higher BFIs (Mwakalila et al., 2002).

411 Comparing to climate attributes, F tends to have smaller effects and with various effects with
412 climate zones (i.e., positive effect in arid and winter rainfall zones). F associates with quick
413 flow generation and thus leads to the changes in the baseflow. The influence comes from
414 vegetation regulation of water flux through moist conditions and E_{TP} (Krakauer and Temimi,
415 2011). The plant on the ground can cover the land surface and influence the E_{TP} and then
416 increase the baseflow. Studies have shown that vegetation cover has a strong control on ET in



417 catchments, and thus influences baseflow generation (Schilling and Libra, 2003). Wittenberg
418 (2003) found that water consumption of deep-rooted vegetation has significant influence on
419 baseflow generation where faster recession is usually found. Furthermore, baseflow is more
420 closely related to the water storage of the saturated zone in plant root zone drainages (Milly,
421 1994). Studies have also shown that higher watershed forest cover usually corresponds well
422 with lower BFI (Price, 2011). This is particularly significant during dry seasons, where the
423 reduction of vegetation cover can lead to increase baseflow in dry seasons (Singh,
424 1968;Price, 2011). In the tropic zone, the proportion of the forest cover within a catchment
425 has negative effect on BFI. This is because of the high water loss through ET in forests, and
426 the vegetation draws heavily on the artesian leakage and contacts the spring flow (Meyboom,
427 1961;Knisel, 1963). Although a relatively close correlation between forest cover and BFI is
428 found for most catchments, there are exceptions in some catchments. For instant, BFI was
429 found to have a weak correlation with forest area in the Mediterranean region (Longobardi
430 and Villani, 2008) and a case study in the Elbe River Basin (Haberlandt et al., 2001).

431 Our study demonstrates that those two topographic features are insignificant impact on the
432 BFI cross Australia, and have different effects on various climate zones (i.e., slope has
433 positive impact on arid but negative on other climate zones). However, some studies found
434 that S and H have positive correlation with the recession timescales (Peña-Arancibia et al.,
435 2010;Krakauer and Temimi, 2011). When interactions crossing level have been implemented,
436 adding those two factors can greatly improve performance of multilevel regression approach.
437 Other studies show that the watershed area and slope are highly associated with the baseflow
438 statistics (Vogel and Kroll, 1992). This can be a result of the catchments in their study are
439 under the 150 km². The effect of the slope will be induced when the catchment area are larger
440 (Peña-Arancibia et al., 2010). However, the study conducted in southeaster Australia found
441 that the topographic parameters have no significant relationship with the BFI (Lacey and



442 Grayson, 1998), this may be groundwater is relatively deep reducing connections between
443 groundwater and streams (Mazvimavi et al., 2005). Besides, Kst is positively related with
444 BFI for all catchment across climate zones. This may be explained by the strong interactions
445 between soil water content and P as well as E_{TP} (Milly, 1994).

446 Our result shows that multilevel regression approach, this approach can better understand the
447 hydrological dynamics within different systems. To be specific, this method considers
448 climate controls on catchment BFIs cross continental scale (Figure 8). Figure 9 shows the
449 different coefficients in each climate zone. The hydrological processes are controlled by
450 various climate conditions at large scale as has been proved by a number of studies (Lacey
451 and Grayson, 1998; Abebe and Foerch, 2006; Merz and Blöschl, 2009; Ahiablame et al., 2013).
452 The baseflow processes will have the interactions at different climate zones (within and
453 between group). The multilevel regression approach considers the cross-level interactions,
454 and the prediction not only influenced by predictors at one scale (i.e., continental scale) but
455 also different spatial scale (i.e., climate zones) (Qian et al., 2010), incorporates the group
456 level information, and this approach takes the fixed and random effects into account one
457 single model, the coefficients of the model for the whole data and the group has the
458 variances. Prediction of BFI using group level information (i.e., climate zones) will help
459 capturing the climate spatial variability at different regional scales.

460 According to the good performance as illustrated above, it is promising that this method can
461 be used as a robust tool to estimate BFI across changing backgrounds (i.e., climate zones),
462 and can promote improved understanding of hydrological processes.

463 **7 Conclusion**

464 This study estimated ensemble baseflow index from four well-parameterised baseflow
465 separation methods (Lyne-Hollick, UKIH (United Kingdom Institute of Hydrology),



466 Chapman-Maxwell and Eckhardt), and found that the baseflow index varies significantly in
467 corresponding to climate zones across Australian continent. Multilevel regression approach is
468 introduced to improve BFI estimate for 596 catchments across Australia. BFI obtained from
469 this new method is compared to that of traditional linear regression method and two
470 hydrological models. When compared to observed BFIs, the multilevel regression approach
471 outperforms both linear regression approach and hydrological models. Traditional linear
472 regression approach fails to considerate the interactions across group levels. The two
473 hydrological models have good performance for simulating runoff yet fail to separate
474 baseflow. In contrast, the multilevel regression approach indicates that annual precipitation,
475 potential evapotranspiration, elevation, land cover and available soil water holding capacity
476 in top part of the soil all have strong control on catchment baseflow, where climate factor
477 including precipitation and potential evapotranspiration are proven to be most significant.
478 The multilevel regression approach can provide insights into the control factors of baseflow
479 generation. This approach has the potential of being used to estimate baseflow index. We
480 proposed the framework of using this approach to estimate hydrological signatures of under
481 various backgrounds.

482 **Author contribution**

483 YQZ conceived this study and conducted rainfall-runoff modelling. JLZ carried out baseflow
484 separation modelling, data analysis and wrote the first version of manuscript. LC, ZKL, PPZ
485 helped modelling. YQZ, JXS, LC, RG, XGS contributed to late versions of paper writing.

486 **Acknowledgments**

487 This study was supported by the National Natural Science Foundation of China (Grant Nos.
488 51379175 and 51679200), Specialized Research Fund for the Doctoral Program of Higher
489 Education (Grant No.20136101110001), Program for Key Science and Technology



490 Innovation Team in Shaanxi Province (Grant No. 2014KCT-27). The first author
491 acknowledges the Chinese Scholarship Council for supporting his Ph.D. Study at CSIRO
492 Land and Water. We thank Nick Potter for his comments and suggestions for an early version
493 of this paper. Data generated from modelling are freely available upon request from the
494 corresponding author (Yongqiang Zhang, email: Yongqiang.zhang@csiro.au). The authors
495 declare no conflict of interest.

496 Competing interests

497 The authors declare that they have no conflict of interest.

498 **References**

- 499 Abdulla, F. A., Lettenmaier, D. P., and Liang, X.: Estimation of the ARNO model baseflow parameters
500 using daily streamflow data, *J. Hydrol.*, 222, 37-54, doi:10.1016/S0022-1694(99)00096-7, 1999.
- 501 Abebe, A., and Foerch, G.: Catchment characteristics as predictors of base flow index (BFI) in
502 Wabishebele river basin, east Africa, Conference on International Agricultural Research for
503 Development, Siegen, Germany, 2006.
- 504 Ahiablame, L., Chaubey, I., Engel, B., Cherkauer, K., and Merwade, V.: Estimation of annual baseflow
505 at ungauged sites in Indiana USA, *J. Hydrol.*, 476, 13-27, doi:10.1016/j.jhydrol.2012.10.002, 2013.
- 506 Arnold, J., Allen, P., Mutiah, R., and Bernhardt, G.: Automated base flow separation and recession
507 analysis techniques, *Groundwater*, 33, 1010-1018, doi:10.1111/j.1745-6584.1995.tb00046.x, 1995.
- 508 Beck, H. E., van Dijk, A. I. J. M., Miralles, D. G., de Jeu, R. A. M., Sampurno Bruijnzeel, L. A.,
509 McVicar, T. R., and Schellekens, J.: Global patterns in base flow index and recession based on
510 streamflow observations from 3394 catchments, *Water Resour. Res.*, 49, 7843-7863,
511 doi:10.1002/2013wr013918, 2013.
- 512 Berk, R. A., and De Leeuw, J.: Multilevel statistical models and ecological scaling, in: *Scaling and*
513 *uncertainty analysis in ecology*, Springer, 67-88, 2006.
- 514 Beven, K., and Freer, J.: Equifinality, data assimilation, and uncertainty estimation in mechanistic
515 modelling of complex environmental systems using the GLUE methodology, *J. Hydrol.*, 249, 11-29,
516 doi:10.1016/S0022-1694(01)00421-8, 2001.
- 517 Bloomfield, J. P., Allen, D. J., and Griffiths, K. J.: Examining geological controls on baseflow index
518 (BFI) using regression analysis: An illustration from the Thames Basin, UK, *J. Hydrol.*, 373, 164-
519 176, doi:10.1016/j.jhydrol.2009.04.025, 2009.
- 520 Brandes, D., Hoffmann, J. G., and Mangarillo, J. T.: Base flow rate, low flows, and hydrologic features
521 of small watersheds in Pennsylvania, USA, *Journal of the American Water Resources Association*,
522 41, 1177-1186, doi:10.1111/j.1752-1688.2005.tb03792.x, 2005.
- 523 Brutsaert, W., and Nieber, J. L.: Regionalized drought flow hydrographs from a mature glaciated
524 plateau, *Water Resour. Res.*, 13, 637-643, doi:10.1029/WR013i003p00637, 1977.
- 525 Brutsaert, W., and Lopez, J. P.: Basin-scale geohydrologic drought flow features of riparian aquifers in
526 the Southern Great Plains, *Water Resour. Res.*, 34, 233-240, doi:10.1029/97WR03068, 1998.
- 527 Brutsaert, W.: *Hydrology: an introduction*, Cambridge University Press, 618 pp., 2005.
- 528 Carey, K.: *Modeling N2O emissions from agricultural soils using a multi-level linear regression*,
529 Citeseer, 2007.



- 530 Chapman, T., and Maxwell, A.: Baseflow separation-comparison of numerical methods with tracer
531 experiments, Hydrology and Water Resources Symposium 1996: Water and the Environment;
532 Preprints of Papers, 1996.
- 533 Cheng, L., Zhang, L., and Brutsaert, W.: Automated selection of pure base flows from regular daily
534 streamflow data: Objective algorithm, *Journal of Hydrologic Engineering*, 21, 06016008,
535 doi:10.1061/(asce)he.1943-5584.0001427, 2016.
- 536 Chiew, F., and McMahon, T.: Application of the daily rainfall-runoff model MODHYDROLOG to 28
537 Australian catchments, *J. Hydrol.*, 153, 383-416, doi:10.1016/0022-1694(94)90200-3, 1994.
- 538 Chiew, F. H. S., and McMahon, T. A.: Modelling the impacts of climate change on Australian
539 streamflow, *Hydrol. Processes*, 16, 1235-1245, doi:10.1002/hyp.1059, 2002.
- 540 Chiew, F. H. S., Teng, J., Vaze, J., Post, D. A., Perraud, J. M., Kirono, D. G. C., and Viney, N. R.:
541 Estimating climate change impact on runoff across southeast Australia: Method, results, and
542 implications of the modeling method, *Water Resour. Res.*, 45, W10414, doi:10.1029/2008wr007338,
543 2009.
- 544 Dudaniec, R. Y., Rhodes, J. R., Worthington Wilmer, J., Lyons, M., Lee, K. E., McAlpine, C. A., and
545 Carrick, F. N.: Using multilevel models to identify drivers of landscape-genetic structure among
546 management areas, *Mol. Ecol.*, 22, 3752-3765, doi:10.1111/mec.12359, 2013.
- 547 Eckhardt, K.: How to construct recursive digital filters for baseflow separation, *Hydrol. Processes*, 19,
548 507-515, doi:10.1002/hyp.5675, 2005.
- 549 Fenicia, F., Savenije, H. H. G., Matgen, P., and Pfister, L.: A comparison of alternative multiobjective
550 calibration strategies for hydrological modeling, *Water Resour. Res.*, 43, n/a-n/a,
551 doi:10.1029/2006WR005098, 2007.
- 552 Ferket, B. V. A., Samain, B., and Pauwels, V. R. N.: Internal validation of conceptual rainfall-runoff
553 models using baseflow separation, *J. Hydrol.*, 381, 158-173, doi:10.1016/j.jhydrol.2009.11.038,
554 2010.
- 555 Friedl, M., Strahler, A., and Hodges, J.: ISLSCP II MODIS (Collection 4) IGBP Land Cover, 2000–
556 2001, ISLSCP Initiative II Collection. Data set. Available on-line [<http://daac.ornl.gov/>] from Oak
557 Ridge National Laboratory Distributed Active Archive Center, Oak Ridge, Tennessee, USA, 10,
558 doi:10.3334/ORNLDAAC/968, 2010.
- 559 Furey, P. R., and Gupta, V. K.: A physically based filter for separating base flow from streamflow time
560 series, *Water Resour. Res.*, 37, 2709-2722, doi:10.1029/2001wr000243, 2001.
- 561 Gallart, F., Latron, J., Llorens, P., and Beven, K.: Using internal catchment information to reduce the
562 uncertainty of discharge and baseflow predictions, *Adv. Water Res.*, 30, 808-823,
563 doi:10.1016/j.advwatres.2006.06.005, 2007.
- 564 Gebert, W. A., Radloff, M. J., Considine, E. J., and Kennedy, J. L.: Use of Streamflow Data to Estimate
565 Base Flow/Ground-Water Recharge For Wisconsin1, *JAWRA Journal of the American Water
566 Resources Association*, 43, 220-236, doi:10.1111/j.1752-1688.2007.00018.x, 2007.
- 567 Gelman, A., and Hill, J.: Data analysis using regression and multilevel/hierarchical models, Cambridge
568 University Press, 2006.
- 569 Gonzales, A., Nonner, J., Heijkers, J., and Uhlenbrook, S.: Comparison of different base flow separation
570 methods in a lowland catchment, *Hydrol. Earth Syst. Sci.*, 13, 2055-2068, doi:10.5194/hess-13-
571 2055-2009, 2009.
- 572 Gustard, A., Bullock, A., and Dixon, J.: Low flow estimation in the United Kingdom, Institute of
573 Hydrology, 1992.
- 574 Gustard, A., and Irving, K.: Classification of the low flow response of European soils, *IAHS
575 Publications-Series of Proceedings and Reports-Intern Assoc Hydrological Sciences*, 221, 113-118,
576 1994.
- 577 Gusyev, M. A., Morgenstern, U., Stewart, M. K., Yamazaki, Y., Kashiwaya, K., Nishihara, T.,
578 Kuribayashi, D., Sawano, H., and Iwami, Y.: Application of tritium in precipitation and baseflow in
579 Japan: a case study of groundwater transit times and storage in Hokkaido watersheds, *Hydrol. Earth
580 Syst. Sci.*, 20, 3043-3058, doi:10.5194/hess-20-3043-2016, 2016.
- 581 Haberlandt, U., Klöcking, B., Krysanova, V., and Becker, A.: Regionalisation of the base flow index
582 from dynamically simulated flow components — a case study in the Elbe River Basin, *J. Hydrol.*,
583 248, 35-53, doi:10.1016/S0022-1694(01)00391-2, 2001.



- 584 Jeffrey, S. J., Carter, J. O., Moodie, K. B., and Beswick, A. R.: Using spatial interpolation to construct
585 a comprehensive archive of Australian climate data, *Environmental Modelling & Software*, 16, 309-
586 330, doi:10.1016/S1364-8152(01)00008-1, 2001.
- 587 Knisel, W. G.: Baseflow recession analysis for comparison of drainage basins and geology, *J. Geophys.*
588 *Res.*, 68, 3649-3653, doi:10.1029/JZ068i012p03649, 1963.
- 589 Koskelo, A. I., Fisher, T. R., Utz, R. M., and Jordan, T. E.: A new precipitation-based method of
590 baseflow separation and event identification for small watersheds (<50km²), *J. Hydrol.*, 450-451,
591 267-278, doi:10.1016/j.jhydrol.2012.04.055, 2012.
- 592 Kottek, M., Grieser, J., Beck, C., Rudolf, B., and Rubel, F.: World Map of the Köppen-Geiger climate
593 classification updated, *Meteorol. Z.*, 15, 259-263, doi:10.1127/0941-2948/2006/0130, 2006.
- 594 Krakauer, N. Y., and Temimi, M.: Stream recession curves and storage variability in small watersheds,
595 *Hydrol. Earth Syst. Sci.*, 15, 2377-2389, doi:10.5194/hess-15-2377-2011, 2011.
- 596 Lacey, G. C., and Grayson, R. B.: Relating baseflow to catchment properties in south-eastern Australia,
597 *J. Hydrol.*, 204, 231-250, doi:10.1016/S0022-1694(97)00124-8, 1998.
- 598 Leuning, R., Zhang, Y. Q., Rajaud, A., Cleugh, H., and Tu, K.: Correction to “A simple surface
599 conductance model to estimate regional evaporation using MODIS leaf area index and the Penman-
600 Monteith equation”, *Water Resour. Res.*, 45, n/a-n/a, doi:10.1029/2008wr007631, 2009.
- 601 Li, H., Zhang, Y., Chiew, F. H. S., and Xu, S.: Predicting runoff in ungauged catchments by using
602 Xinanjiang model with MODIS leaf area index, *J. Hydrol.*, 370, 155-162,
603 doi:10.1016/j.jhydrol.2009.03.003, 2009.
- 604 Li, H., and Zhang, Y.: Regionalising rainfall-runoff modelling for predicting daily runoff in continental
605 Australia, *Hydrol. Earth Syst. Sci. Discuss.*, 1-24, doi:10.5194/hess-2016-464, 2016.
- 606 Li, H., and Zhang, Y.: Regionalising rainfall-runoff modelling for predicting daily runoff: Comparing
607 gridded spatial proximity and gridded integrated similarity approaches against their lumped
608 counterparts, *J. Hydrol.*, 550, 279-293, doi:10.1016/j.jhydrol.2017.05.015, 2017.
- 609 Lo, M.-H., Yeh, P. J. F., and Famiglietti, J. S.: Constraining water table depth simulations in a land
610 surface model using estimated baseflow, *Adv. Water Res.*, 31, 1552-1564,
611 doi:10.1016/j.advwatres.2008.06.007, 2008.
- 612 Longobardi, A., and Villani, P.: Baseflow index regionalization analysis in a mediterranean area and
613 data scarcity context: Role of the catchment permeability index, *J. Hydrol.*, 355, 63-75,
614 doi:10.1016/j.jhydrol.2008.03.011, 2008.
- 615 Lott, D. A., and Stewart, M. T.: Base flow separation: A comparison of analytical and mass balance
616 methods, *J. Hydrol.*, 535, 525-533, doi:10.1016/j.jhydrol.2016.01.063, 2016.
- 617 Lü, H., Hou, T., Horton, R., Zhu, Y., Chen, X., Jia, Y., Wang, W., and Fu, X.: The streamflow
618 estimation using the Xinanjiang rainfall runoff model and dual state-parameter estimation method,
619 *J. Hydrol.*, 480, 102-114, doi:10.1016/j.jhydrol.2012.12.011, 2013.
- 620 Luo, Y., Arnold, J., Allen, P., and Chen, X.: Baseflow simulation using SWAT model in an inland river
621 basin in Tianshan Mountains, Northwest China, *Hydrol. Earth Syst. Sci.*, 16, 1259-1267,
622 doi:10.5194/hess-16-1259-2012, 2012.
- 623 Luo, Z., Wang, E., and Smith, C.: Fresh carbon input differentially impacts soil carbon decomposition
624 across natural and managed systems, *Ecology*, 96, 2806-2813, doi:10.1890/14-2228.1, 2015.
- 625 Lyne, V., and Hollick, M.: Stochastic time-variable rainfall-runoff modelling, Institute of Engineers
626 Australia National Conference, 1979.
- 627 MathWorks, T.: Genetic algorithm and direct search toolbox 2 user's guide, pp. 5.2-5.13, Natick, Mass.,
628 2006.
- 629 Mazvimavi, D., Meijerink, A. M. J., Savenije, H. H. G., and Stein, A.: Prediction of flow characteristics
630 using multiple regression and neural networks: A case study in Zimbabwe, *Physics and Chemistry*
631 *of the Earth, Parts A/B/C*, 30, 639-647, doi:10.1016/j.pce.2005.08.003, 2005.
- 632 McMahon, S. M., and Diez, J. M.: Scales of association: hierarchical linear models and the
633 measurement of ecological systems, *Ecol. Lett.*, 10, 437-452, doi:10.1111/j.1461-
634 0248.2007.01036.x, 2007.
- 635 Merz, R., and Blöschl, G.: A regional analysis of event runoff coefficients with respect to climate and
636 catchment characteristics in Austria, *Water Resour. Res.*, 45, W01405, doi:10.1029/2008wr007163,
637 2009.



- 638 Meyboom, P.: Estimating ground-water recharge from stream hydrographs, *J. Geophys. Res.*, 66, 1203-
639 1214, doi:10.1029/JZ066i004p01203, 1961.
- 640 Meynink, W.: Modelling equatorial baseflow, Proceedings of the 34th World Congress of the
641 International Association for Hydro-Environment Research and Engineering: 33rd Hydrology and
642 Water Resources Symposium and 10th Conference on Hydraulics in Water Engineering, 2011.
- 643 Miller, M. P., Susong, D. D., Shope, C. L., Heilweil, V. M., and Stolp, B. J.: Continuous estimation of
644 baseflow in snowmelt-dominated streams and rivers in the Upper Colorado River Basin: A chemical
645 hydrograph separation approach, *Water Resour. Res.*, 50, 6986-6999, doi:10.1002/2013WR014939,
646 2014.
- 647 Miller, M. P., Buto, S. G., Susong, D. D., and Rumsey, C. A.: The importance of base flow in sustaining
648 surface water flow in the Upper Colorado River Basin, *Water Resour. Res.*, 3547–3562,
649 doi:10.1002/2015WR017963, 2016.
- 650 Milly, P. C. D.: Climate, soil water storage, and the average annual water balance, *Water Resour. Res.*,
651 30, 2143-2156, doi:10.1029/94WR00586, 1994.
- 652 Mwakalila, S., Feyen, J., and Wyseure, G.: The influence of physical catchment properties on baseflow
653 in semi-arid environments, *J. Arid Environ.*, 52, 245-258, doi:10.1006/jare.2001.0947, 2002.
- 654 Nash, J. E., and Sutcliffe, J. V.: River flow forecasting through conceptual models part I — A discussion
655 of principles, *J. Hydrol.*, 10, 282-290, doi:10.1016/0022-1694(70)90255-6 1970.
- 656 Partington, D., Brunner, P., Simmons, C. T., Werner, A. D., Therrien, R., Maier, H. R., and Dandy, G.
657 C.: Evaluation of outputs from automated baseflow separation methods against simulated baseflow
658 from a physically based, surface water-groundwater flow model, *J. Hydrol.*, 458-459, 28-39,
659 doi:10.1016/j.jhydrol.2012.06.029, 2012.
- 660 Peña-Arancibia, J. L., van Dijk, A. I. J. M., Mulligan, M., and Bruijnzeel, L. A.: The role of climatic
661 and terrain attributes in estimating baseflow recession in tropical catchments, *Hydrol. Earth Syst.*
662 *Sci.*, 14, 2193-2205, doi:10.5194/hess-14-2193-2010, 2010.
- 663 Piggott, A. R., Moin, S., and Southam, C.: A revised approach to the UKIH method for the calculation
664 of baseflow, *Hydrol. Sci. J.*, 50, doi:10.1623/hysj.2005.50.5.911, 2005.
- 665 Price, K.: Effects of watershed topography, soils, land use, and climate on baseflow hydrology in humid
666 regions: A review, *Progress in Physical Geography*, 35, 465-492, doi:10.1177/0309133311402714,
667 2011.
- 668 Qian, S. S., Cuffney, T. F., Alameddine, I., McMahon, G., and Reckhow, K. H.: On the application of
669 multilevel modeling in environmental and ecological studies, *Ecology*, 91, 355-361, doi:10.1890/09-
670 1043.1, 2010.
- 671 Rice, K. C., and Hornberger, G. M.: Comparison of hydrochemical tracers to estimate source
672 contributions to peak flow in a small, forested, headwater catchment, *Water Resour. Res.*, 34, 1755-
673 1766, doi:10.1029/98WR00917, 1998.
- 674 Santhi, C., Allen, P. M., Muttiah, R. S., Arnold, J. G., and Tuppad, P.: Regional estimation of base flow
675 for the conterminous United States by hydrologic landscape regions, *J. Hydrol.*, 351, 139-153,
676 doi:10.1016/j.jhydrol.2007.12.018, 2008.
- 677 Schilling, K. E., and Libra, R. D.: INCREASED BASEFLOW IN IOWA OVER THE SECOND HALF
678 OF THE 20TH CENTURY1, *JAWRA Journal of the American Water Resources Association*, 39,
679 851-860, doi:10.1111/j.1752-1688.2003.tb04410.x, 2003.
- 680 Singh, K. P.: Some Factors Affecting Baseflow, *Water Resour. Res.*, 4, 985-999,
681 doi:10.1029/WR004i005p00985, 1968.
- 682 Spongberg, M.: Spectral analysis of base flow separation with digital filters, *Water Resour. Res.*, 36,
683 745-752, doi:10.1029/1999WR900303, 2000.
- 684 Stoelzle, M., Weiler, M., Stahl, K., Morhard, A., and Schuetz, T.: Is there a superior conceptual
685 groundwater model structure for baseflow simulation?, *Hydrol. Processes*, 29, 1301-1313,
686 doi:10.1002/hyp.10251, 2015.
- 687 Su, C.-H., Peterson, T. J., Costelloe, J. F., and Western, A. W.: A synthetic study to evaluate the utility
688 of hydrological signatures for calibrating a base flow separation filter, *Water Resour. Res.*, 6526-
689 6540, doi:10.1002/2015WR018177, 2016.
- 690 Tularam, G. A., and Ilahee, M.: Exponential smoothing method of base flow separation and its impact
691 on continuous loss estimates, *American Journal of Environmental Sciences*, 4, 373-381,
692 doi:10.3844/ajessp.2008.136.144, 2008.



- 693 van Dijk, A. I. J. M.: Climate and terrain factors explaining streamflow response and recession in
694 Australian catchments, *Hydrol. Earth Syst. Sci.*, 14, 159-169, doi:10.5194/hess-14-159-2010, 2010.
- 695 van Dijk, A. I. J. M., Peña-Arancibia, J. L., Wood, E. F., Sheffield, J., and Beck, H. E.: Global analysis
696 of seasonal streamflow predictability using an ensemble prediction system and observations from
697 6192 small catchments worldwide, *Water Resour. Res.*, 49, 2729-2746, doi:10.1002/wrcr.20251,
698 2013.
- 699 Vaze, J., and Teng, J.: Future climate and runoff projections across New South Wales, Australia: results
700 and practical applications, *Hydrol. Processes*, 25, 18-35, doi:10.1002/hyp.7812, 2011.
- 701 Vogel, R. M., and Kroll, C. N.: Regional geohydrologic-geomorphic relationships for the estimation of
702 low-flow statistics, *Water Resour. Res.*, 28, 2451-2458, doi:10.1029/92WR01007, 1992.
- 703 Wittenberg, H., and Sivapalan, M.: Watershed groundwater balance estimation using streamflow
704 recession analysis and baseflow separation, *J. Hydrol.*, 219, 20-33, doi:10.1016/S0022-
705 1694(99)00040-2, 1999.
- 706 Wittenberg, H.: Effects of season and man-made changes on baseflow and flow recession: case studies,
707 *Hydrol. Processes*, 17, 2113-2123, doi:10.1002/hyp.1324, 2003.
- 708 Yao, C., Zhang, K., Yu, Z., Li, Z., and Li, Q.: Improving the flood prediction capability of the
709 Xinanjiang model in ungauged nested catchments by coupling it with the geomorphologic
710 instantaneous unit hydrograph, *J. Hydrol.*, 517, 1035-1048, doi:10.1016/j.jhydrol.2014.06.037, 2014.
- 711 Zhang, J., Zhang, Y., Song, J., and Cheng, L.: Evaluating relative merits of four baseflow separation
712 methods in Eastern Australia, *J. Hydrol.*, 549, 252-263, doi:10.1016/j.jhydrol.2017.04.004, 2017.
- 713 Zhang, Y., and Chiew, F. H. S.: Relative merits of different methods for runoff predictions in ungauged
714 catchments, *Water Resour. Res.*, 45, W07412, doi:10.1029/2008wr007504, 2009.
- 715 Zhang, Y., Leuning, R., Hutley, L. B., Beringer, J., McHugh, I., and Walker, J. P.: Using long-term
716 water balances to parameterize surface conductances and calculate evaporation at 0.05° spatial
717 resolution, *Water Resour. Res.*, 46, W05512, doi:10.1029/2009wr008716, 2010.
- 718 Zhang, Y., Viney, N., Frost, A., Oke, A., Brooks, M., Chen, Y., and Campbell, N.: Collation of
719 Australian modeller's streamflow dataset for 780 unregulated Australian catchments, *Water for a
720 Healthy Country National Research Flagship*, 115pp. *Catchment Management*,
721 doi:10.4225/08/58b5baad4fcc2, 2013.
- 722 Zhang, Y., Zheng, H., Chiew, F. H. S., Arancibia, J. P., and Zhou, X.: Evaluating regional and global
723 hydrological models against streamflow and evapotranspiration measurements, *Journal of
724 Hydrometeorology*, 17, 995-1010, doi:10.1175/jhm-d-15-0107.1, 2016.
- 725 Zhang, Y. Q., Vaze, J., Chiew, F. H., Teng, J., and Li, M.: Predicting hydrological signatures in
726 ungauged catchments using spatial interpolation, index model, and rainfall-runoff modelling, *J.
727 Hydrol.*, 517, 936-948, doi:10.1016/j.jhydrol.2014.06.032, 2014.
- 728 Zhao, R. J.: The Xinanjiang model applied in China, *J. Hydrol.*, 135, 371-381, doi:10.1016/0022-
729 1694(92)90096-E, 1992.
- 730 Zhu, Z., Bi, J., Pan, Y., Ganguly, S., Anav, A., Xu, L., Samanta, A., Piao, S., Nemani, R., and Myneni,
731 R.: Global Data Sets of Vegetation Leaf Area Index (LAI)3g and Fraction of Photosynthetically
732 Active Radiation (FPAR)3g Derived from Global Inventory Modeling and Mapping Studies
733 (GIMMS) Normalized Difference Vegetation Index (NDVI3g) for the Period 1981 to 2011, *Remote
734 Sensing*, 5, 927-948, doi:10.3390/rs5020927, 2013.



735 **Figure captions**

736 Figure 1. The location of 596 selected unregulated small catchments in this study and climate
737 classification based on Köppen-Geiger (2006) classification schemes in Australia.

738 Figure 2. Estimation of the recession constant ($\text{Log}(-dQ/dt)$ versus $\text{log}(Q)$) using automated
739 baseflow identification technique (ABIT) for Endeavour catchment (station ID 107001). The
740 black line is 5 % lower envelope line has a slope 0.983 and the estimate of the characteristic
741 drainage time scale $K = 57.1$ days.

742 Figure 3. Spatial distribution of the observed baseflow index across Australia.

743 Figure 4. Baseflow index duration curves obtained from the observed, SIMHYD model and
744 Xinanjiang model. Calibration and two regionalisation results are shown for each
745 hydrological model, where R1 and R2 represent spatial proximity and integrated similarity
746 approaches, respectively. SIMHYD is simplified version of the HYDROLOG model.

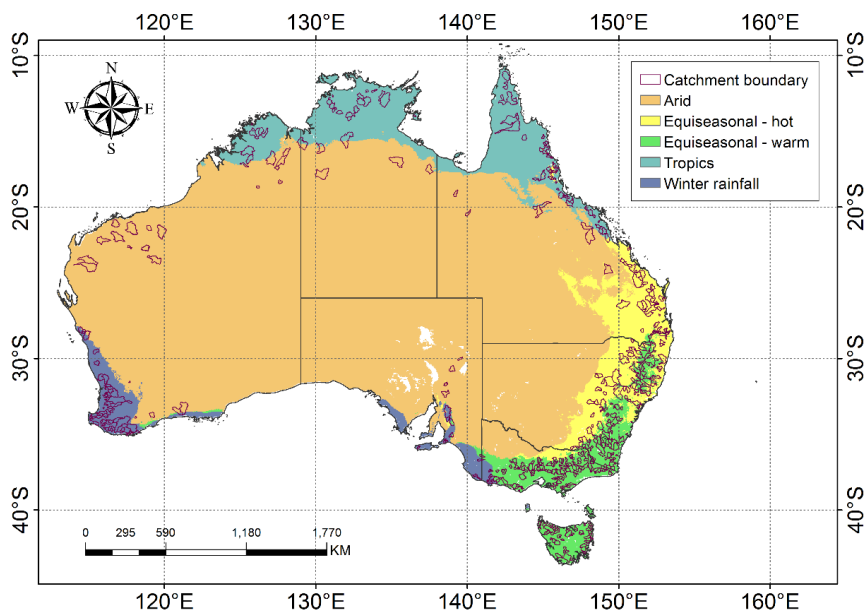
747 Figure 5. Scatterplots of observed baseflow index versus simulated baseflow index using
748 SIMHYD and Xinanjiang models, where calibrated and regionalised model results are
749 presented in (a) and (d) (calibration), (b) and (e) (spatial proximity regionalisation) and (c)
750 and (f) (integrated similarity regionalisation), respectively. The blue ellipses represent the
751 confidence level at 0.95. The full naming of SIMHYD is introduced in Figure 4.

752 Figure 6. Scatterplots of observed and simulated baseflow index using traditional linear
753 regression ((a)-(d)) and multilevel regression ((e)-(f)) approaches that are built using the full
754 catchment samples in four climate zones, with (a) and (e) for arid, (b) and (f) for tropics, (c)
755 and (g) for equiseasonal and (d) and (h) for winter rainfall, respectively. The blue ellipse is
756 drawn at 0.95 confidence level. The black line represents 1:1 line.

757 Figure 7. As same as Figure 6, but using the leave-one-out cross validation approach.



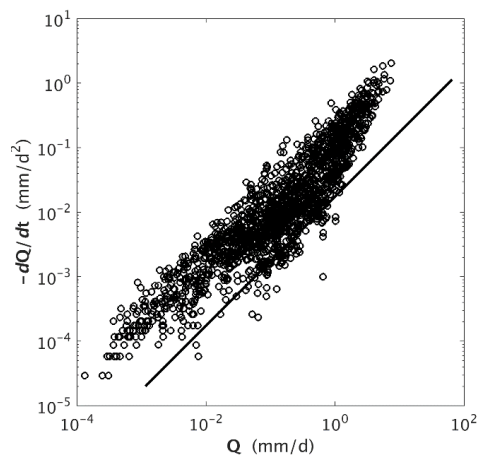
758 Figure 8. Parameter values using multilevel regression approach, fixed and random variables
759 are represented. Error bar represents standard error of each parameter. The abbreviations of
760 catchment attributes are introduced in Table 1.



761

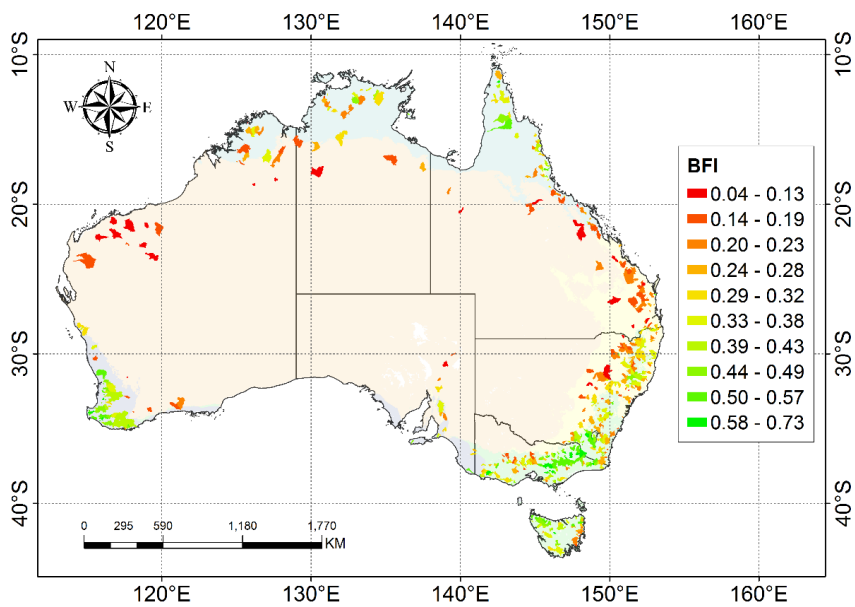
762 Figure 1. The location of 596 selected unregulated small catchments in this study and climate

763 classification based on Köppen-Geiger (2006) classification schemes in Australia.



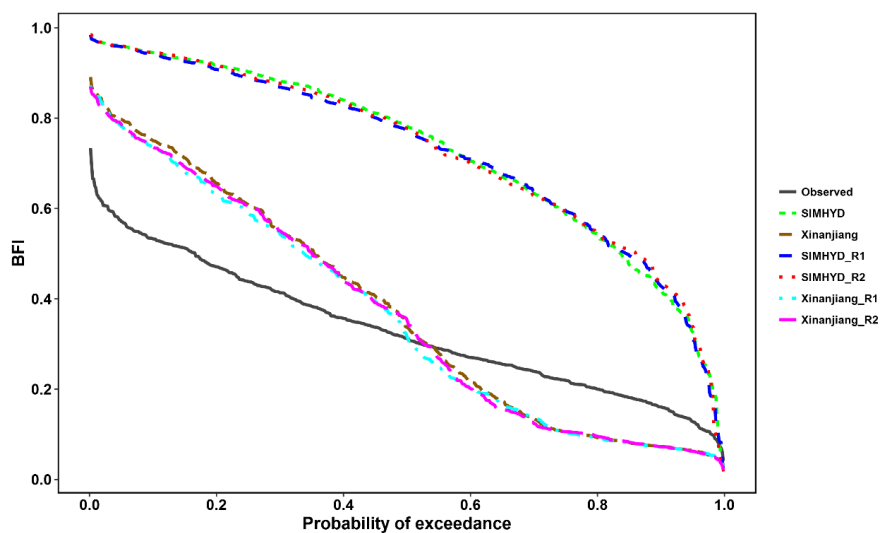
764

765 Figure 2. Estimation of the recession constant ($\text{Log}(-dQ/dt)$ versus $\text{log}(Q)$) using automated
766 baseflow identification technique (ABIT) for Endeavour catchment (station ID 107001). The
767 black line is 5 % lower envelope line has a slope 0.983 and the estimate of the characteristic
768 drainage time scale $K = 57.1$ days.



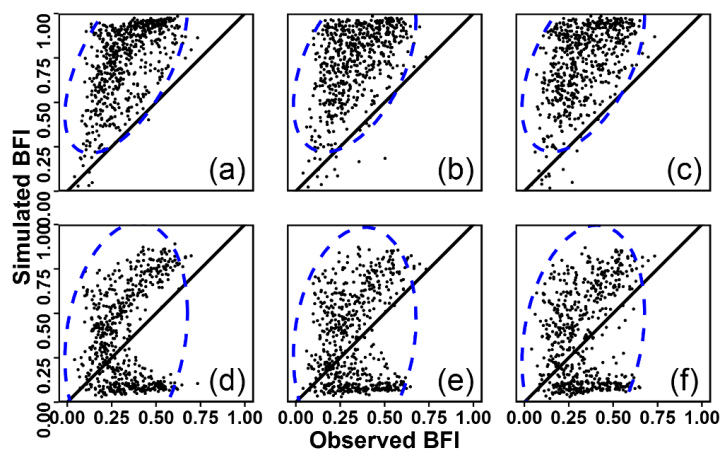
769

770 Figure 3. Spatial distribution of the observed baseflow index across Australia.



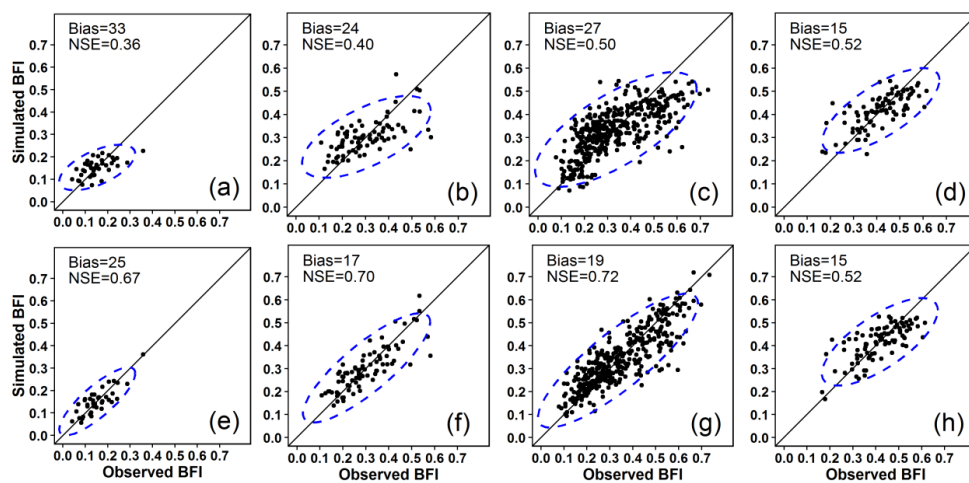
771

772 Figure 4. Baseflow index duration curves obtained from the observed, SIMHYD model and
773 Xinanjiang model. Calibration and two regionalisation results are shown for each
774 hydrological model, where R1 and R2 represent spatial proximity and integrated similarity
775 approaches, respectively. SIMHYD is simplified version of the HYDROLOG model.



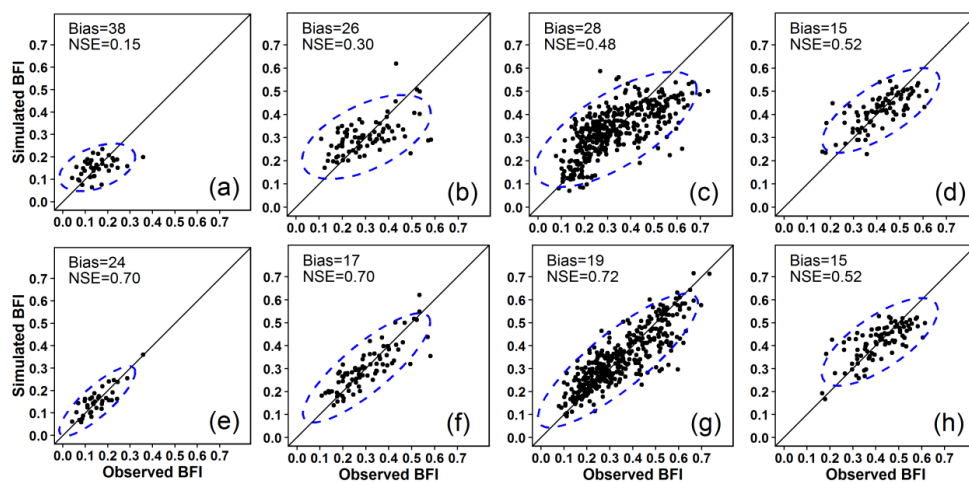
776

777 Figure 5. Scatterplots of observed baseflow index versus simulated baseflow index using
778 SIMHYD and Xinanjiang models, where calibrated and regionalised model results are
779 presented in (a) and (d) (calibration), (b) and (e) (spatial proximity regionalisation) and (c)
780 and (f) (integrated similarity regionalisation), respectively. The blue ellipses represent the
781 confidence level at 0.95. The full naming of SIMHYD is introduced in Figure 4.



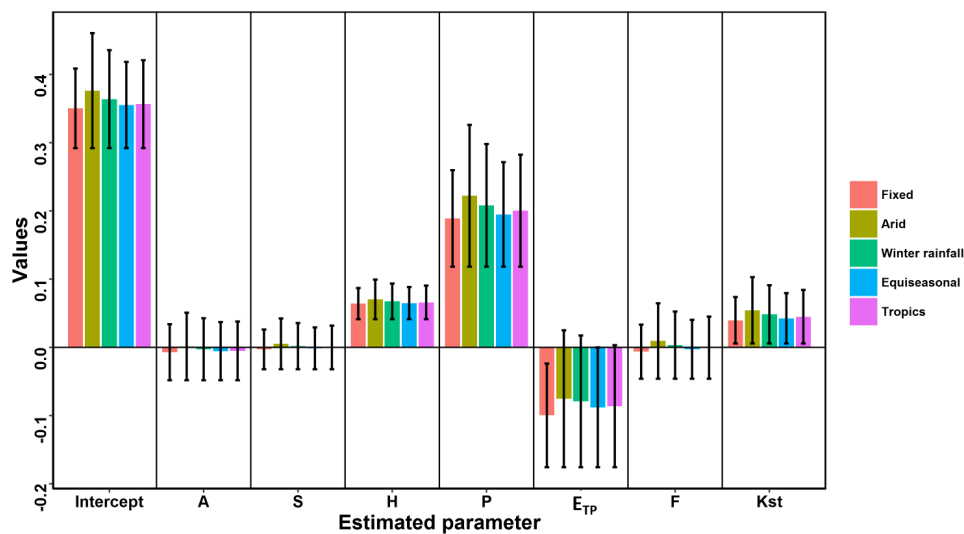
782

783 Figure 6. Scatterplots of observed and simulated baseflow index using traditional linear
784 regression ((a)-(d)) and multilevel regression ((e)-(f)) approaches that are built using the full
785 catchment samples in four climate zones, with (a) and (e) for arid, (b) and (f) for tropics, (c)
786 and (g) for equiseasonal and (d) and (h) for winter rainfall, respectively. The blue ellipse is
787 drawn at 0.95 confidence level. The black line represents 1:1 line.



788

789 Figure 7. As same as Figure 6, but using the leave-one-out cross validation approach.



790

791 Figure 8. Parameter values using multilevel regression approach, fixed and random variables
792 are represented. Error bar represents standard error of each parameter. The abbreviations of
793 catchment attributes are introduced in Table 1.



794 Table 1. Catchment attributes and indicators used in present study

Catchment attributes	Notation	Unit
Area	A	km ²
Mean elevation	H	m
Mean slope	S	%
Mean annual precipitation	P	mm a ⁻¹
Mean annual potential evaporation	E_{TP}	mm a ⁻¹
Forest cover ratio	F	%
Available soil water holding capacity in top soil	K_{st}	mm/hr

795



796 Table 2. Summary statistics of the catchments information including topographic, climate,
797 geological elements and forest cover ratio in 596 catchments across Australia. The
798 abbreviations of catchment attributes are introduced in Table 1.

	A	H	S	P	E _{TP}	F	Kst
Max	4805.93	1350.97	16.02	3683.76	2237.88	0.91	507.28
Min	50.34	37.61	0.15	241.77	905.88	0.01	5.54
Mean	646.06	433.21	4.48	981.12	1384.12	0.49	158.83
25th	153.31	223.18	1.90	727.42	1155.48	0.34	105.42
50th	346.15	347.00	3.60	885.32	1294.93	0.52	161.17
75th	710.13	604.29	6.71	1162.30	1536.10	0.67	201.90

799



800 Table 3. Using various benchmarks to evaluate prediction of baseflow index from traditional
 801 linear and multilevel regression approaches. Ensemble is mean of four revised methods(LH,
 802 UKIH, CM and ECK are the revised methods of Lyne-Hollick, United Kingdom Institute of
 803 Hydrology, Chapman-Maxwell and Eckhardt methods respectively). Details of each method
 804 can be found in [Zhang *et al.*, 2017].

Method		Ensemble	LH	UKIH	CM	ECK
Linear	Bias	25	23	114	18	113
	NSE	0.57	0.25	0.49	0.33	0.37
Multilevel	Bias	19	21	111	17	102
	NSE	0.75	0.41	0.65	0.38	0.55

805